USBL/INS INTEGRATION TECHNIQUE FOR UNDERWATER VEHICLES

M. Morgado P. Oliveira C. Silvestre
J.F. Vasconcelos [1]

IST - Instituto Superior Técnico
ISR - Institute for Systems and Robotics
Av. Rovisco Pais, 1, 1049-001, Lisbon, Portugal
{marcomorgado,pjcro,cjs,jfvasconcelos}@isr.ist.utl.pt

Abstract: This paper presents an Ultra-Short Baseline (USBL) and Inertial Navigation System (INS) integration technique to enhance position and orientation estimates of underwater vehicles. Two closed-form methods for the computation of the position of aiding transponders are presented and compared, exploiting the planar approximation of the acoustic waves or considering the distances between the transponders and receivers, respectively. As the distance between the transponder and receivers increases, similar performance for both positioning methods is evidenced. Enhanced performance of the overall USBL/INS aided navigation system is assessed in simulation.

Keywords: USBL, INS, Underwater positioning, Underwater navigation

1. INTRODUCTION

During the last decade, the use of Underwater Vehicles (UV) to accomplish several tasks at sea, including environmental monitoring, surveillance, underwater inspection of estuaries, harbors, and pipelines, and geological and biological surveys (Pascoal *et al.*, 2000), has grown considerably. The fulfillment of these missions often requires low-cost, compact, high performance, robust positioning and navigation systems that can accurately estimate the UV position and orientation.

Classical positioning solutions resort to Ultra-short baseline (USBL) systems (Vickery, 1998), consisting of small and compact arrays of acoustic transducers. Pre-calibrated configurations allow for the measurements of the direction of arrival of acoustic signals emitted by a transponder and its range. Due to the velocity of acoustic waves in the water, multi-path phenomena, and other disturbances, these systems can only provide measurements at very low update rates (typically inferior to 1 Hz), with a performance that degrades as the transponder/USBL distance increases. When coupled to attitude estimation units, composed by inclinometers and fluxgate compasses, vehicle position and orientation in a Earth fixed reference coordinate frame can be computed. However, this solution does not meet typical underwater navigational accuracy requirements.

This paper proposes a coupled USBL/Inertial Navigation System navigation architecture to enhance the accuracy and update rates on the vehicle's position and orientation estimates. Inertial

[1] This work was partially supported by Fundação para a Ciência e a Tecnologia (ISR/IST pluriannual funding) through the POS_Conhecimento Program that includes FEDER funds and by the project PDCT/MAR/55609/2004 - RUMOS of the FCT. The work of J.F. Vasconcelos and M. Morgado was supported by PhD Student Scholarships, SFRH/BD/18954/2004 and SFRH/BD/25368/2005, respectively, from the Portuguese FCT POCTI programme.

Navigation Systems (INS) provide self-contained passive means for the computation of three-dimensional position and attitude estimates, with excellent short-term accuracy. Due to uncompensated rate gyro and accelerometer errors and nonlinear disturbances the INS accuracy degrades over time. The USBL/INS sensor fusion is accomplished by using an Extended Kalman Filter (EKF) implemented in a direct feedback configuration (Brown and Hwang, 1997).

The USBL acoustic array is installed onboard the underwater vehicle, with a topology known as inverted USBL (Vickery, 1998), and interrogates transponders located at known positions of the vehicle's mission scenario. See an alternative solution in (Steinke and Buckham, 2005).

The paper is organized as follows: in Section 2, two closed-form methods of estimating the transponders position are introduced. Section 3 discusses the adopted USBL/INS navigation architecture and derives the observation equations for the USBL/INS integration strategy. Comparison results of both methods for transponders position estimation and performance analysis of the overall navigation system are presented in Section 4. Finally, Section 5 provides concluding remarks on the subject and comments on future work.

2. USBL POSITIONING METHODS

This section presents two closed-form methods of estimating the transponders positions in a reference coordinate frame. In the first method, the position of the transponders is computed resorting to the planar approximation of the acoustic waves (Yli-Hietanen *et al.*, 1996), here on referred to as the Planar Wave (PW) method. The latter is based on the equation error formulation presented in (Smith and Abel, 1987), referred to as the Equation Error (EE) method.

The determination of round trip travel time and the respective stochastic characterization are obtained resorting to pulse detection matched filters of acoustic signals modulated using spread-spectrum CDMA techniques (Austin, 1994). Two type of errors are identified: the first, common to all receivers, includes transponder-receiver relative motion time-scaling effects (Doppler effects and others) and errors in sound propagation velocity; the second, corresponds to the differential quantization error induced by the acoustic system sampling frequency and the digital implementation of the detection algorithms.

2.1 Planar Wave positioning method

For realistic mission scenarios of underwater vehicles the distances between receivers are much

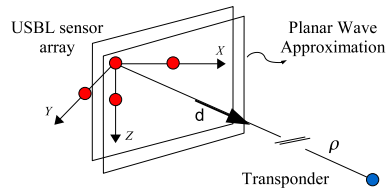

Fig. 1. Planar Wave method

smaller than the distances between the sensor array and the transponders, thus the planar wave approximation for the acoustic waves is valid. The PW method is based on that approximation to obtain the range and direction of the transponders. The position is then computed in Body coordinate frame. Consider the planar wave, the USBL sensor array, and the transponder depicted in Fig. 1. The measurement of travel time is obtained from the round trip travel time of the acoustic signals between the USBL array and the transponder. Taking into account the quantization performed by the acoustic system, the travel time measurements for receiver i are given by

$$t_i = T_s \left[\frac{\bar{t}_i + \varepsilon_c}{T_s} \right] \tag{1}$$

where $\bar{t}_i$ is the nominal travel time, ε_c represents the common mode noise for transponder j, T_s is the acoustic sampling period and $[\cdot]$ represents the mathematical *round* operator. Along the derivation the index j will be omitted. The travel time measurements are considered to be approximately described by

$$t_i = \bar{t}_i + \eta_i \tag{2}$$

where η_i represents the measurement noise for receiver i.

Taking into account the planar wave approximation, the Time Difference Of Arrival (TDOA) between receivers i and k is given by

$$\delta^{(i,k)} = t_i - t_k = -\frac{1}{v_p}\mathbf{d}' \left({}^{B}\bar{\mathbf{p}}_{r_i} - {}^{B}\bar{\mathbf{p}}_{r_k} \right) \tag{3}$$

where v_p is the speed of sound in the water, ${}^{B}\mathbf{p}_{r_g}$ is receiver g ($g \in \{i,k\}$) position on Body frame and $\mathbf{d}$ is the unit direction vector of transponder j ($\|\mathbf{d}\|_2 = 1$).

The vector of TDOA between all possible combinations of N receivers is described, from (3) $\{i = 1,\ldots,N; k = 1,\ldots,N; i \neq k\}$, by

$$\boldsymbol{\Delta} = \left[\delta^{(1,2)} \;\; \delta^{(1,3)} \;\; \cdots \;\; \delta^{(N-1,N)} \right]'$$

and it can be generated by

$$\boldsymbol{\Delta} = \mathbf{C}\,\mathbf{t}$$

where $\mathbf{C}$ is a combination matrix and $\mathbf{t}$ is the vector of time measurements from all receivers defined as $\mathbf{t} = \left[t_1 \;\; t_2 \;\; \cdots \;\; t_N \right]'$.

Considering that $\mathbf{t}$ is disturbed by zero mean noise of equal intensity for all receivers, the least squares solution for the transponder's j direction $\mathbf{d}$ is

$$\mathbf{d} = -v_p \mathbf{S}^{\#} \mathbf{C}\,\mathbf{t}$$

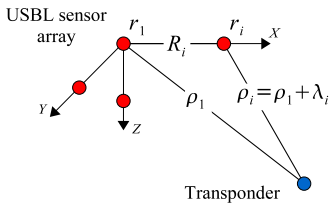

Fig. 2. Equation Error method

where $\mathbf{S}^{\#}$ is the pseudo-inverse of $\mathbf{S}$ given by

$$\mathbf{S}^{\#} = (\mathbf{S}'\mathbf{S})^{-1}\mathbf{S}' \ , \ \mathbf{S} = \begin{bmatrix} {}^{B}\bar{\mathbf{p}}'_{r_1} - {}^{B}\bar{\mathbf{p}}'_{r_2} \\ {}^{B}\bar{\mathbf{p}}'_{r_1} - {}^{B}\bar{\mathbf{p}}'_{r_3} \\ \vdots \\ {}^{B}\bar{\mathbf{p}}'_{r_{N-1}} - {}^{B}\bar{\mathbf{p}}'_{r_N} \end{bmatrix}$$

Also resorting to the planar wave approximation, the range of the transponder to the origin of Body frame can be computed by averaging the range estimates from all receivers. The estimate for receiver h ($h \in \{1,\ldots,N\}$) is computed from

$$\rho_h = v_p t_h + {}^{B}\bar{\mathbf{p}}'_{r_h}\,\mathbf{d} \qquad (4)$$

Thus, averaging (4) for all N receivers yields

$$\rho = \frac{1}{N}\sum_{h=1}^{N}\left(v_p t_h + {}^{B}\bar{\mathbf{p}}'_{r_h}\,\mathbf{d}\right)$$

Finally, the relative position of the j^{th} transponder, expressed in Body frame, is computed by

$${}^{B}\mathbf{p}_{e_j m} = \rho_j\,\mathbf{d}_j$$

2.2 Equation Error positioning method

The Equation Error (EE) method is based on the equation error formulation presented in (Smith and Abel, 1987). This method computes directly the position of the transponders in Body frame without using the planar approximation. Consider the USBL sensor array and the transponder depicted in Fig. 2. The relations between the transponder e_j, the reference receiver r_1 located at the origin of the Body frame, and another receiver r_i ($i \neq 1$) can be easily established:

$$\rho_1 = \| {}^{B}\mathbf{p}_{e_j} \| \ , \ \rho_i = \| {}^{B}\bar{\mathbf{p}}_{r_i} - {}^{B}\mathbf{p}_{e_j} \|$$

$$\rho_i = \rho_1 + \lambda_i \qquad (5)$$

$$\rho_i^2 = R_i^2 - 2\,{}^{B}\bar{\mathbf{p}}'_{r_i}\,{}^{B}\mathbf{p}_{e_j} + \rho_1^2 \qquad (6)$$

where ρ_i is the distance between the transponder and receiver r_i, R_i is the distance between reference receiver r_1 and receiver r_i, and λ_i is the Range Difference Of Arrival (RDOA) between receiver r_i and the reference receiver r_1. Replacing (5) in (6) yields

$$R_i^2 - \lambda_i^2 - 2\rho_1\lambda_i - 2\,{}^{B}\bar{\mathbf{p}}'_{r_i}\,{}^{B}\mathbf{p}_{e_j} = 0 \qquad (7)$$

The RDOA measurements must verify the constraint imposed by (7). Due to the noise present in the measurements a constraint violation variable is introduced in (7), according to the so called Equation Error (Smith and Abel, 1987). Thus,

$$R_i^2 - \lambda_i^2 - 2\rho_1\lambda_i - 2\,{}^{B}\bar{\mathbf{p}}'_{r_i}\,{}^{B}\mathbf{p}_{e_j} = \epsilon_i \qquad (8)$$

where ϵ_i is the constraint violation variable for the receiver r_i. Considering

$$\boldsymbol{\delta} = \begin{bmatrix} R_2^2 - \lambda_2^2 \\ R_3^2 - \lambda_3^2 \\ \vdots \\ R_N^2 - \lambda_N^2 \end{bmatrix} \qquad \boldsymbol{\epsilon} = \begin{bmatrix} \epsilon_2 \\ \epsilon_3 \\ \vdots \\ \epsilon_N \end{bmatrix}$$

$$\boldsymbol{\Lambda} = \begin{bmatrix} \lambda_2 \\ \lambda_3 \\ \vdots \\ \lambda_N \end{bmatrix} \qquad \mathbf{T} = \begin{bmatrix} {}^{B}\bar{\mathbf{p}}'_{r_2} \\ {}^{B}\bar{\mathbf{p}}'_{r_3} \\ \vdots \\ {}^{B}\bar{\mathbf{p}}'_{r_N} \end{bmatrix}$$

the set of $N-1$ equations is given in matrix notation by

$$\boldsymbol{\epsilon} = \boldsymbol{\delta} - 2\rho_1\boldsymbol{\Lambda} - 2\mathbf{T}\,{}^{B}\mathbf{p}_{e_j}$$

To compute the position of the transponder in Body frame, the least squares solution obtained from minimizing the constraint violation energy $J = \boldsymbol{\epsilon}'\boldsymbol{\epsilon}$ is given by

$${}^{B}\mathbf{p}_{e_j m} = \frac{1}{2}\mathbf{T}^{\#}\left(\boldsymbol{\delta} - 2\rho_1\boldsymbol{\Lambda}\right)$$

where $\mathbf{T}^{\#}$ is the pseudo-inverse of $\mathbf{T}$. Notice that as in the PW method, the set $\boldsymbol{\Lambda}$ of RDOA measurements can be obtained from $\boldsymbol{\Lambda} = v_p\mathbf{C}\mathbf{t}$.

3. USBL/INS INTEGRATION ARCHITECTURE

This section briefly describes the navigation system architecture adopted in this work and derives the equations that allow for the compensation of the disturbances and errors that occur in the INS and the USBL positioning system. Both systems complement each other: the USBL low update rates and accuracy are compensated by the high rates and excellent short-term accuracy of the INS; the long term unbounded errors inherent to a dead-reckoning INS are compensated by the USBL position fixes.

3.1 INS direct-feedback architecture

The INS performs attitude, velocity and position numerical integration from rate gyro and accelerometer triads data, rigidly mounted on the vehicle structure (strapdown configuration). The non-ideal inertial sensor effects due to noise and bias are dynamically compensated by the EKF that estimates position, velocity, attitude and bias compensation errors. The inertial errors are compensated according to the direct-feedback configuration depicted in Fig. 3. The INS

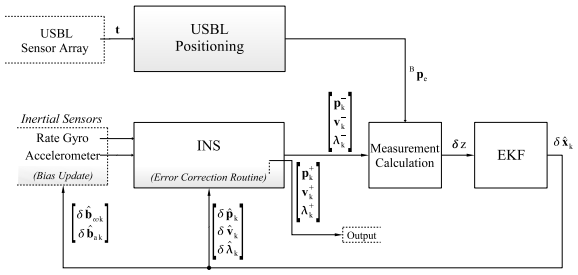

Fig. 3. Navigation System Block Diagram

multi-rate approach, based on the work detailed in (Savage, 1998*a*; Savage, 1998*b*), computes the dynamic angular rate/acceleration effects using high-speed, low order algorithms, whose output is periodically fed to a moderate-speed algorithm that computes attitude/velocity resorting to exact, closed-form equations. The numerical integration performed by the INS algorithms takes into account the angular, velocity and position high-frequency motions, referred to as coning, sculling, and scrolling respectively, to avoid estimation errors buildup.

The inputs provided to the inertial algorithms are the accelerometer and rate gyro readings, corrupted by zero mean white noise $\mathbf{n}$ and random walk bias, $\dot{\mathbf{b}} = \mathbf{n}_b$, yielding

$$^B\mathbf{a}_{SF} = {}^B\,\bar{\mathbf{a}} + {}^B\,\bar{\mathbf{g}} - \delta\mathbf{b}_a + \mathbf{n}_a, \quad \boldsymbol{\omega} = \bar{\boldsymbol{\omega}} - \delta\mathbf{b}_\omega + \mathbf{n}_\omega$$

where $\delta\mathbf{b} = \mathbf{b} - \bar{\mathbf{b}}$ denotes bias compensation error, $\bar{\mathbf{b}}$ is the nominal bias, $\mathbf{b}$ is the compensated bias, ${}^B\bar{\mathbf{g}}$ is the nominal gravity vector, and the subscripts a and ω identify accelerometer and rate gyro quantities, respectively.

The moderate-speed inertial algorithms attitude output is represented in Direction Cosine Matrix (DCM) form, and velocity and position are expressed in Earth frame coordinates, $\mathbf{v}$ and $\mathbf{p}$ respectively. For further details on the INS algorithm adopted in this work, see (Morgado *et al.*, 2006) and the references therein.

The EKF error equations, based on perturbational rigid body kinematics, were brought to full detail by Britting (Britting, 1971), and are applied to local navigation by modeling the position, velocity, attitude and bias compensation errors dynamics, respectively

$$\begin{aligned}
\delta\dot{\mathbf{p}} &= \delta\mathbf{v} \\
\delta\dot{\mathbf{v}} &= -\mathcal{R}\delta\mathbf{b}_a - [\mathcal{R}^B\mathbf{a}_{SF}\times]\delta\boldsymbol{\lambda} + \mathcal{R}\mathbf{n}_a \\
\delta\dot{\boldsymbol{\lambda}} &= -\mathcal{R}\delta\mathbf{b}_\omega + \mathcal{R}\mathbf{n}_\omega \\
\delta\dot{\mathbf{b}}_a &= -\mathbf{n}_{b_a} \\
\delta\dot{\mathbf{b}}_\omega &= -\mathbf{n}_{b_\omega}
\end{aligned}$$

where the position and velocity linear errors are defined, respectively by

$$\delta\mathbf{p} = \mathbf{p} - \bar{\mathbf{p}}\ ,\ \delta\mathbf{v} = \mathbf{v} - \bar{\mathbf{v}}, \tag{9}$$

matrix $\mathcal{R}$ is the shorthand notation for Body to Earth coordinate frames rotation matrix, ${}^E_B\mathbf{R}$, and the attitude error rotation vector $\delta\boldsymbol{\lambda}$ is defined by $\mathbf{R}(\delta\boldsymbol{\lambda}) = \mathcal{R}\bar{\mathcal{R}}'$ and bears a first order approximation

$$\mathbf{R}(\delta\boldsymbol{\lambda}) \simeq \mathbf{I}_{3\times3} + [\delta\boldsymbol{\lambda}\times] \Rightarrow [\delta\boldsymbol{\lambda}\times] \simeq \mathcal{R}\bar{\mathcal{R}}' - \mathbf{I}_{3\times3} \tag{10}$$

of the Direction Cosine Matrix (DCM), where $\bar{\mathcal{R}}$ represents nominal rotation matrix.

The EKF error estimates are fed into the INS error correction routines as depicted in Fig. 3. The attitude estimate, $\mathcal{R}_k^-$, is compensated using the rotation error matrix $\mathbf{R}(\delta\boldsymbol{\lambda})$ definition, which yields

$$\mathcal{R}_k^+ = \mathbf{R}'_k(\delta\hat{\boldsymbol{\lambda}}_k)\mathcal{R}_k^-$$

where $\mathbf{R}'_k(\delta\hat{\boldsymbol{\lambda}}_k)$ is parameterized by the rotation vector $\delta\hat{\boldsymbol{\lambda}}_k$ according to the DCM form. The remaining state variables are linearly compensated using

$$\begin{aligned}
\mathbf{p}_k^+ &= \mathbf{p}_k^- - \delta\hat{\mathbf{p}}_k \quad , \quad \mathbf{v}_k^+ = \mathbf{v}_k^- - \delta\hat{\mathbf{v}}_k \\
\mathbf{b}_{a\ k}^+ &= \mathbf{b}_{a\ k}^- - \delta\hat{\mathbf{b}}_{a\ k}\ , \ \mathbf{b}_{\omega\ k}^+ = \mathbf{b}_{\omega\ k}^- - \delta\hat{\mathbf{b}}_{\omega\ k}
\end{aligned}$$

After the error correction procedure is completed, the EKF error estimates are reset and the filter linearization assumptions remain valid.

3.2 USBL integration with the INS

The set of equations that allows for the integration of the INS with the USBL positioning system is derived by comparison of the transponders position fixes supplied by the USBL with the estimates provided by the INS. The resulting measurement residual equation is then expressed in terms of the EKF state variables and implemented according to the direct-feedback structure presented in Fig. 3.

The position of a transponder in Body frame can be described by

$${}^B\mathbf{p}_{e_j m} = \bar{\mathcal{R}}'\left({}^E\bar{\mathbf{p}}_{e_j} - \bar{\mathbf{p}}\right) + \mathbf{n}_{pr} \tag{11}$$

where ${}^E\bar{\mathbf{p}}_{e_j}$ is the transponder's position in Earth coordinate frame, $\bar{\mathbf{p}}$ is the nominal position of the Body frame origin in Earth frame and $\mathbf{n}_{pr}$ represents the relative position measurement noise, characterized by taking into account the acoustic sensors noises and the USBL positioning system.

The estimate of the relative position of the transponder j in Body frame can be computed using the INS *a priori* estimates $\mathcal{R}$ and $\mathbf{p}$, as follows

$${}^B\mathbf{p}_{e_j} = \mathcal{R}'\left({}^E\bar{\mathbf{p}}_{e_j} - \mathbf{p}\right)$$

Using the position error definition (9), replacing the rotation matrix $\bar{\mathcal{R}}$ by the attitude error $\delta\boldsymbol{\lambda}$ approximation (10), and ignoring second order error terms, manipulation of (11) yields

$${}^B\mathbf{p}_{e_j m} = {}^B\mathbf{p}_{e_j} + \mathcal{R}'\delta\mathbf{p} - \left[{}^B\mathbf{p}_{e_j}\times\right]\mathcal{R}'\delta\boldsymbol{\lambda} + \mathbf{n}_{pr}$$

The measurement residual used as observation in the EKF is given by the comparison between the measured and the estimated relative positions, leading to

$$\delta \mathbf{z}_{pr} = {}^{B}\mathbf{p}_{e_j m} - {}^{B}\mathbf{p}_{e_j} = \mathcal{R}'\delta\mathbf{p} - \left[\, {}^{B}\mathbf{p}_{e_j} \times \right] \mathcal{R}'\delta\boldsymbol{\lambda} + \mathbf{n}_{pr}$$

The sensor fusion methodology presented here is based on the classical approach that relies on solving separately the positioning and the sensor fusion problems. A different approach is presented in (Morgado *et al.*, 2006), in which the positioning system is directly embedded in the EKF allowing to enhance estimation errors.

Observability analysis revealed that either stopped or along a straight line path, full observability is only achieved using at least three transponders (on a non-singular geometry) or two transponders and a magnetometer for attitude error compensation. Moreover, along curves two transponders or one transponder and a magnetometer are sufficient to achieve full observability. In light of this results, Earth magnetic field readings provided by an onboard magnetometer extra aiding device, are included in the proposed solution. For further details on the observability analysis and the inclusion of the magnetometer extra aiding device, see (Morgado *et al.*, 2006).

4. SIMULATION RESULTS

In this section, both USBL positioning methods are compared using Monte-Carlo runs and the INS/USBL navigation system is assessed in simulation. The comparison of both methods is achieved through 1000 Monte-Carlo runs for each position of the transponder and using a USBL sensor array with five receivers in the configuration depicted in Fig. 4. The acoustic sensors are considered to be disturbed by zero mean Additive White Gaussian Noise (AWGN) with a variance of $(50\mu s)^2$ prior to the quantization procedure (note that this AWGN is the same for all receivers and that the differential disturbance is induced by the quantization). The quantization was performed with a sampling frequency of 400 kHz.

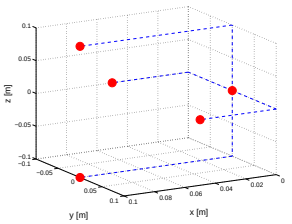

Fig. 4. Receivers installation geometry

The Root Mean Square (RMS) of the position error norm of both positioning methods is presented in Fig. 5, varying the position of the transponder from $[0.1, 0, 0]'$ m to $[15, 0, 0]'$ m. As expected,

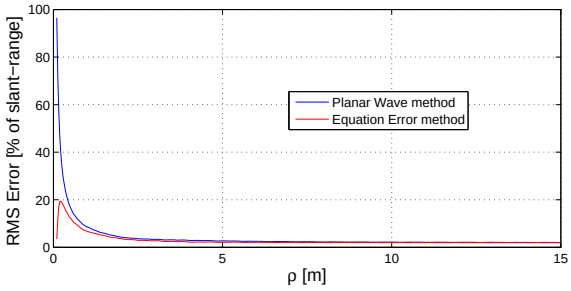

Fig. 5. RMS error of position estimates

in the close-range area of the sensor array, up to about 5 meters, the EE method performs better than the PW method. As the distance between the transponder and the USBL array increases, the performance of both methods converges to around 2% of the slant-range of the transponder. It is important to remark that the performance of the USBL positioning strategies is highly dependent on the sampling frequency of the acoustic system. Higher sampling frequency translates into lower uncertainty induced by the quantization process. Thus, the performance of the acoustic system can be much improved, either by increasing the sampling frequency to the limits of performance imposed by the sampling process, or through interpolation techniques since the bandwidth of the acoustic signals and the acoustic transducers is known.

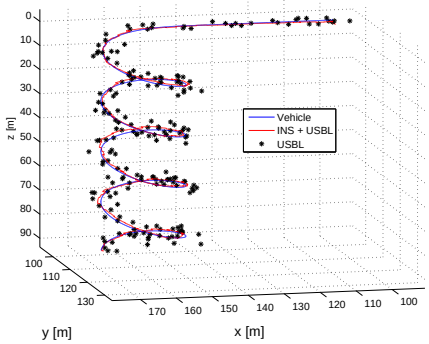

Fig. 6. Vehicle trajectory and USBL/INS results

The performance of the overall navigation system was assessed in simulation using one magnetometer, five receivers installed on the vehicle, in the configuration depicted in Fig. 4 and one single transponder located at the origin of the Earth coordinate frame. The PW method was used for USBL positioning of the transponder, since for the considered distances between the transponder and the USBL array both methods hold similar results. Moreover, the EE method involves quadratic terms of the TDOA measurements which are very small, in the order of microseconds, inducing additional errors related to numerical precision and representation.

The covariance matrix of the noise vector of the acoustic receivers $\boldsymbol{\eta} = \begin{bmatrix} \eta_1 & \cdots & \eta_N \end{bmatrix}'$ was charac-

Table 1. Sensor errors

Sensor	Bias	Noise Variance
Rate gyro	0.05 °/s	$(0.02\ °/s)^2$
Accelerometer	10 mg	$(0.6\ \text{mg})^2$
Magnetometer	-	$(1\ \mu\text{G})^2$

terized through extensive Monte-Carlo runs. The INS high-speed algorithm is set to run at 100 Hz and the normal-speed algorithm is synchronized with the EKF, both executed at 50 Hz. The USBL array provides measurements at 1 Hz. The white Gaussian noise and bias characteristics of the sensors are presented in Table 1.

The vehicle follows a trajectory composed by a initial straight line with non-null acceleration followed by a descending helix represented in Fig. 6 together with the overall navigation system results and the USBL position fixes (after correctly rotated to the Earth frame by $\mathbf{p} = {}^{E}\bar{\mathbf{p}}_{e_j} - \overline{\mathcal{R}}\,{}^{B}\mathbf{p}_{e_j m}$). The USBL/INS navigation system starts with an initial position estimation error of 5 meters on the y and z components. The position estimation errors of the USBL/INS navigation system are depicted in Fig. 7 and summarized in Table 2 where the performance enhancement is obvious.

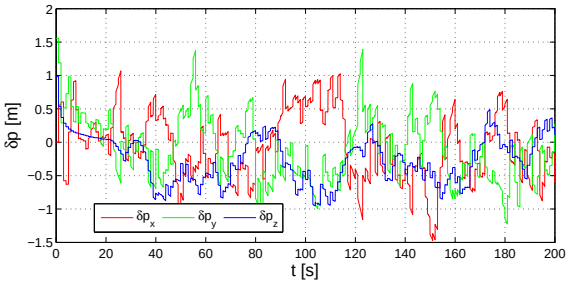

Fig. 7. Position estimation errors

Table 2. Position estimation errors (RMS)

	$\boldsymbol{\delta p_x}$ [m]	$\boldsymbol{\delta p_y}$ [m]	$\boldsymbol{\delta p_z}$ [m]
USBL (1 Hz)	2.1986	2.3923	1.5256
INS/USBL (50 Hz)	0.5051	0.4996	0.4385

5. CONCLUSIONS

Two closed-form methods of estimating transponders positions using USBL arrays were presented and compared. One of the methods exploits the planar approximation of the acoustic waves whereas the other method directly exploits the euclidean distances between the receivers and the transponders. From the simulation results it became clear that as the distance between transponders and the USBL array increases, both methods converge to the same performance level. Simulation results also evidenced the USBL/INS integration enhancement in position estimates and at higher rates than the standalone USBL solution. Future work will focus on field test characterization of the round trip travel time error sources and on the implementation of the proposed architecture in a low-power consumption DSP hardware setup.

REFERENCES

Austin, T.C. (1994). The application of spread spectrum signaling techniques to underwater acoustic navigation. In: *Proceedings of the 1994 Symposium on Autonomous Underwater Vehicle Technology, 1994. AUV '94.*

Britting, K.R. (1971). *Inertial Navigation Systems Analysis*. John Wiley & Sons, Inc.

Brown, R.G. and P.Y.C. Hwang (1997). *Introduction to Random Signals and Applied Kalman Filtering*. third ed.. John Wiley & Sons.

Morgado, M., P. Oliveira, C. Silvestre and J.F. Vasconcelos (2006). USBL/INS Tightly-Coupled Integration Technique for Underwater Vehicles. In: *Proceedings Of The 9th International Conference on Information Fusion*. Florence, Italy.

Pascoal, A., P. Oliveira and C. Silvestre *et al.* (2000). Robotic Ocean Vehicles for Marine Science Applications: the European ASIMOV Project. In: *Proceedings of the Oceans 2000*. Rhode Island, USA.

Savage, P.G. (1998*a*). Strapdown Inertial Navigation Integration Algorithm Design Part 1: Attitude Algorithms. *AIAA Journal of Guidance, Control, and Dynamics* **21**(1), 19–28.

Savage, P.G. (1998*b*). Strapdown Inertial Navigation Integration Algorithm Design Part 2: Velocity and Position Algorithms. *AIAA Journal of Guidance, Control, and Dynamics* **21**(2), 208–221.

Smith, J.O. and J.S. Abel (1987). The Spherical Interpolation Method of Source Localization. *IEEE Journal of Oceanic Engineering* **12**(1), 246–252.

Steinke, D.M. and B.J. Buckham (2005). A Kalman filter for the navigation of remotely operated vehicles. In: *Proceedings of the MTS/IEEE OCEANS 2005*. Washington, DC, USA.

Vickery, K. (1998). Acoustic positioning systems. New concepts - The future. In: *Proceedings Of The 1998 Workshop on Autonomous Underwater Vehicles, AUV'98*. Cambridge, MA, USA.

Yli-Hietanen, J., K. Kalliojarvi and J. Astola (1996). Low-Complexity Angle of Arrival Estimation of Wideband Signals Using Small Arrays. In: *Proceedings 8th IEEE Signal Processing Workshop on Statistical Signal and Array Processing*.